Heliyon 10 (2024) e24690

Contents lists available at ScienceDirect

Heliyon

journal homepage: www.cell.com/heliyon

Research article

Synthesis of nickel particles for use in nickel/silicone rubber composites for the application of electromagnetic interference shielding gaskets

Atefeh Heidarian [a], Hamed Naderi-Samani [b,*], Reza Shoja Razavi [b], Mahsa Nejad Jabbari [b], Ehsan Naderi-Samani [b]

[a] Faculty of Materials and Metallurgical Engineering, Amirkabir University of Technology, Iran
[b] Faculty of Materials and Manufacturing Technologies, Malek Ashtar University of Technology, Iran

ARTICLE INFO

Keywords:
EMI gaskets
Conductive gaskets
Shielding effectiveness
Silicone rubber

ABSTRACT

The effectiveness of electromagnetic interference (EMI) shielding is valuable for construction materials and can be enhanced by the addition of nickel particles to silicone rubber. This investigation reports the chemical reduction process employed to produce nickel powders. The resulting powders were analyzed through SEM imaging and X-ray diffraction analysis, which indicated the production of crystalline, pure nickel powders with spherical morphology. Subsequently, the study delves into nickel filler content enhances the shielding effectiveness (1.2–2.6 GHz) of gaskets by increasing the absorption loss SEA, due to the increase in electrical conductivity. The experimentation was conducted using three samples, revealing that increasing the weight percentage of filler from 30 to 70 % resulted in a considerable reduction in electrical resistivity to 0.6 Ω cm. Moreover, the shielding effectiveness was observed to increased to above 55 dBm when tested across a frequency range of 1.2–2.6 GHz.

1. Introduction

Nowadays, with increasing people's demands for a convenient life, more electrical and electronic equipment are produced. However, this equipment caused hazards because of electromagnetic interference pollution (EMI) and electronic plastic waste. On the other hand, electronic devices are used for communication, computation, and automation increases the working capability, but intentional sources of EMI like Wi-Fi, Bluetooth, etc., have affected the lifetime and efficiency of electronic and electrical devices; also harmful influences in the human body, causing neurological disorders, and uncontrolled behavior [1,2].

Recent advancements in the electronics industry have led to miniaturization and rapid growth in consumer electronics devices. Long-term exposure to some of these devices can cause unintentional harm to humans. The primary concern with these electronic devices is the emission of electromagnetic waves (EMW) that could also interfere with the functionality of other electronic devices. The phenomenon of EMWs causing disruptions to the functionality of another electronic device is known as electromagnetic interference (EMI). The concept of EMI is not new, as there have been numerous reports of blackouts caused by EMI in power grids due to lightning and disruptions to the functionality of satellites orbiting earth due to solar storms. Extensive research done in Europe has found that prolonged exposure to EMWs can cause adverse effects on an infant's brain development and in some cases, could lead to carcinogenic

* Corresponding author.
E-mail address: h.naderi@mut.ac.ir (H. Naderi-Samani).

https://doi.org/10.1016/j.heliyon.2024.e24690
Received 5 September 2023; Received in revised form 24 December 2023; Accepted 12 January 2024

conditions. Medical devices such as cardiac pacemakers are known to malfunction due to EMI, which may even lead to the demise of the individual wearing them. Another worrisome EMI in recent times is created by the detonation of a nuclear device that would fry entire electronic circuitry ceasing the functionality of multiple electronic systems [3,4].

EMI shielding is the technique employed to prevent electromagnetic radiation from penetrating electronic devices through specialized materials that can both absorb and reflect this type of radiation, typically in the radio wave and microwave frequency ranges. The primary objective of EMI shielding is to safeguard electronic appliances such as computers and transformers from the harmful effects of electric fields that can disrupt the electron flow in these devices, thereby compromising their functionality. By acting as a physical barrier to the penetration of electromagnetic radiation, EMI shielding is an essential protective measure. To protect electronic devices from traces of electromagnetic waves, absorbents like conductive gaskets and conductive enclosures are usual. These materials, because of their high electrical conductivity, generate induced current using an injected external electromagnetic field. This phenomenon, protects electronic equipment as indicated in shielding theory and is named shielding effectiveness (SE) [5].

Furthermore, properties such as suitable mechanical strength, low electrical resistivity and weight, resistance against various temperatures, moisture, etc., are essential. These properties are obtained by distributing silver, copper, iron, nickel, cobalt, zinc, aluminum, magnesium, etc., as metallic fillers in a polymeric matrix. Magnetic materials are attractive for shielding, due to their ability to shield by the radiation absorption. The absorption behavior stems from the interaction of the AC magnetic field in electromagnetic radiation with the magnetic dipoles present in the magnetic material. A well-known magnetic material with an exceptionally high magnetic permeability is mumetal, which is nickel [2].

Nickel was chosen due to its ferromagnetic character and its common use as a metallic filler. Copper is another material that is used for increasing the conductivity of polymers. Copper is more conductive than nickel, but it is not magnetic and is inferior in oxidation resistance. Due to the conductivity and magnetic permeability provided by the nickel particles, a comparison of the electromagnetic behavior of the polymer-based materials with and without filler is expected to reveal the science of the electromagnetic behavior. Metallic fillers absorb, reflect and transmit electromagnetic waves and reduce their destructive effects. It should be noted that protective materials cannot wholly remove the impacts of waves but also decline them by redirecting magnetic fields. When conductive fillers are exposed to magnetic fields, electrons and holes interact with the field by orientation, so good electrical conductivity of fillers is essential [6].

Common polymeric matrices used in conductive gaskets are silicone rubber, fluorosilicone and Ethylene Propylene Diene Monomer (EPDM). Features of the suitable matrix are the capability to mold, impenetrability against moisture and air, neutral versus acid, oil and temperature. By comparing different matrices, it concluded that silicone rubber is the best choice. One of the significant advantages of silicone rubber is easy forming by conventional mold pressing or extrusion process that leads to mold gaskets in different and complex shapes [7,8].

Therefore, developing new materials with excellent shielding effectiveness, lightweight, low cost and good conductivity is still a significant challenge. To deal with this challenge, various polymers with numerous fillers are expanded.

In this paper, first, nickel particles were synthesized by chemical reduction for use as a filler. Then, gaskets were prepared by mixing nickel with silicone rubber. Finally, the electrical resistivity and SE properties of gaskets were studied.

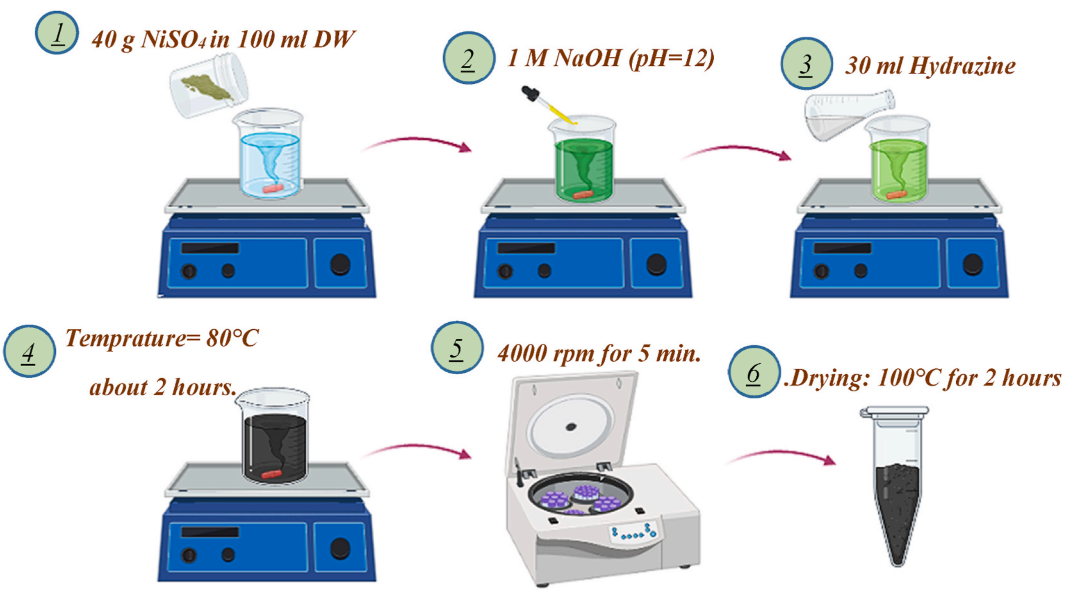

Fig. 1. Nickel synthesis process.

2. Materials

Pure and conductive nickel powder was prepared by a chemical process. To synthesize the nickel powders, nickel sulfate ($NiSO_4$, Merck, purity>99 %), sodium hydroxide (NaOH, Merck, purity>99 %), hydrazine (N_2H_4, Merck, purity>99 %) and ethanol were used. High temperature vulcanizing silicone rubber (HTV, HRS, Korea) and crosslinking agent (peroxide, HRS, Korea) were used to produced conductive gaskets.

2.1. Preparation of nickel particles

To prepare nickel particles as a filler in gaskets, 40 g of $NiSO_4$ was added to 100 ml of distilled water and stirred to form a green, transparent solution. Next, a 1 M solution of NaOH was added slowly and continuously stirred until the solution reached a pH of 12.30 ml hydrazine, as a reducing agent, was added to the mixture. The temperature was maintained at 80 °C during the deposition process. The resulting deposition was centrifuged at 4000 rpm for 5 min and washed with ethanol before being dried in an oven at 100 °C for 2 h. The only challenge of this process could be a complete reduction of nickel particles due to its low purity in raw materials such as $NiSO_4$. The synthesis process can be viewed in Fig. 1.

2.2. Conductive silicone rubber gasket preparation

This study aimed to fabricate conductive gaskets by incorporating silicon rubbers, crosslinking agents and fillers at different weight percentages (30, 50 and 70 %) via planetary mixing equipment. Subsequently, the obtained conductive paste was pressed into a 600 × 300 × 3 mm^3 stainless steel mold with a pressure of 10 MPa and maintained at 185 °C for 10 min.

2.3. Characterization

To examine the pure phase identification, x-ray diffraction (XRD: Philips PW1730, Cu k_α, $\lambda = 1.54060$ Å) with step size = 0.05 at room temperature was used. The morphological study was carried out via scanning electron microscope (Tescan, Mira III). The electrical conductivity was measured by four point probe resistivity meter and the coaxial transmission line method, according to ASTM ES-7-83, was used to measure the EMI shielding effectiveness (SE). The SE was evaluated by measuring the attenuation or reduction of the electromagnetic waves by the shield in the frequency range from 1200 to 2600 MHz.

3. Result and discussion

3.1. Characterization of nickel particles

3.1.1. X-ray diffraction pattern

Fig. 2 illustrates the x-ray diffraction (XRD) patterns of nickel particles, which validate the successful synthesis of a pure crystalline phase of nickel. The XRD peaks at $2\theta = 44.48$, 51.94, and 76.42 are characteristic of the (111), (200), and (220) crystalline planes, respectively (JCPDS card no.01-1260), and correspond to the expected face-centered cubic structure of nickel powder. As such, the synthesis method produced nickel particles of high purity without any impurities [9,10].

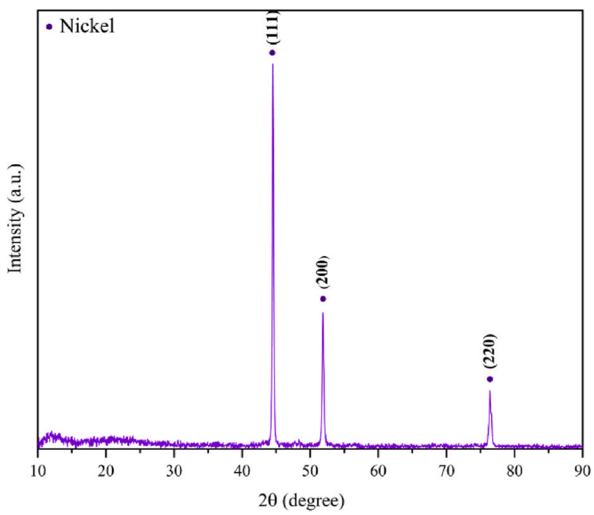

Fig. 2. XRD pattern of pure synthesized nickel.

3.1.2. Morphological observation

The data represented in Fig. 3(a) reveals the predominant circular morphology of the nickel particles, characterized by an average grain size valuing about 0.68 μm. A thorough analysis of 50 distinct grain diameters confirmed a slight standard deviation of 0.25, suggesting a minimal variation in particle size distribution [11]. Also, the EDS graph in Fig. 3(b) confirms pure nickel was synthesized.

3.2. Evaluating conductive gaskets

3.2.1. Surface analysis

In the realm of polymer composites, achieving a successful dispersion and distribution of filler particles is mainly contingent upon compatibility between the filler and matrix. The conductivity of gaskets, hinges on the quality of aggregation and distribution of conductive fillers and their interaction with the matrix. Consequently, the development of conductive gaskets requires optimal polymer-filler interaction, which can be facilitated by the incorporation of a crosslinking agent into the silicone rubber and filler particle mixture. Visual evidence of this successful interaction can be observed through scanning electron microscope (SEM) images of samples containing varying concentrations of filler particles (i.e., 30 wt%, 50 wt% and 70 wt%), as depicted in Fig. 4(a–c). Tellingly, these SEM images demonstrate a roughened surface of the conductive gaskets, increasing the contact area. These findings are supported and further validated by the EDS graphs in Fig. 4(a_1-c_1), which reveal the weight percentages of certain elements. Of particular note is the observed increase in nickel content, which aligns with and affirms the visual data gleaned from SEM images [8].

3.2.2. Electrical resistivity

Fig. 5 depicts the correlation between nickel loading and volume resistivity in silicone rubber composites. The volume resistivity of specimens with a 30 % weight percent of nickel ranged at approximately 23 Ω cm. As the filler loading was raised from 30 % to 50 % by weight, a reduction in volume resistivity to 7 Ω cm was observed. Upon increasing the loading to 70 % by weight and achieving the percolation threshold, a significant drop in volume resistivity to 0.6 Ω cm was evident. This volume resistivity is obtained by the dispersion of nickel particles through a polymer matrix. Polymer played a glue role and connected particles to each other causing electrical conductivity. Additionally, SEM images of samples containing 30 %, 50 %, and 70 % weight percent of nickel revealed a silicone rubber matrix with effective dispersion and distribution of nickel particles. Generally, the electro-conductivity of silicon-filled polymer is decided by the uniform distribution and large aspect ratio of nickel at its content lower than 70 wt%. However, the dispersion of nickel is a crucial factor for the electrical conductivity of polymer/nickel composites at its content higher than 70 wt% [12].

3.2.3. Shielding effectiveness

Fig. 6 indicates the variation in shielding effectiveness (SE) of conductive gaskets within the frequency range of 1200–2600 MHz. The SE exhibited a positive correlation with the filler loadings, as illustrated in figure. A sample containing 30 wt% filler had the lowest SE due to its poor volume resistivity. However, increasing the filler concentration resulted in higher shielding effectiveness. The SE exceeded 55 dBm across the entire frequency range when the nickel loading was 70 wt% Moreover, a direct correlation was observed between the volume resistivity and SE. This is due to the enhanced electrical interaction in the presence of the nickel particles, and the particularly enhanced magnetic interaction at low frequencies [10]. A decrease in volume resistivity led to a lower electromagnetic impedance of the composite and a higher level of impedance mismatch to air. Additionally, increasing filler loadings led to a more compact structure, which narrowed the gap between fillers and matrix and resulted in optimum interfacial polarization of an electromagnetic wave and more significant electromagnetic loss. Hence, the SE of conductive gaskets relied on resistance and interfacial polarization loss [13,14].

The S-parameters, or scattering parameters, describe how a network with N ports responds to signals incoming at one or more of its

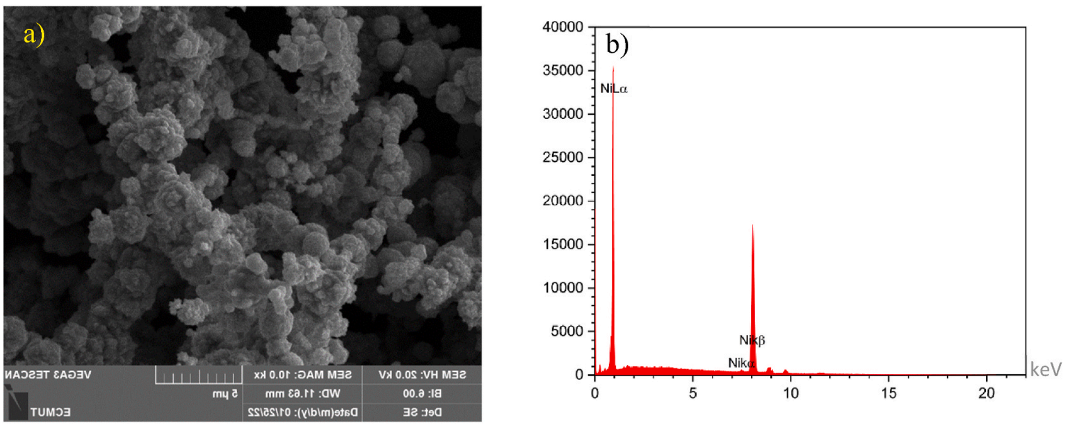

Fig. 3. a) SEM image and b) EDS graph of pure synthesized nickel.

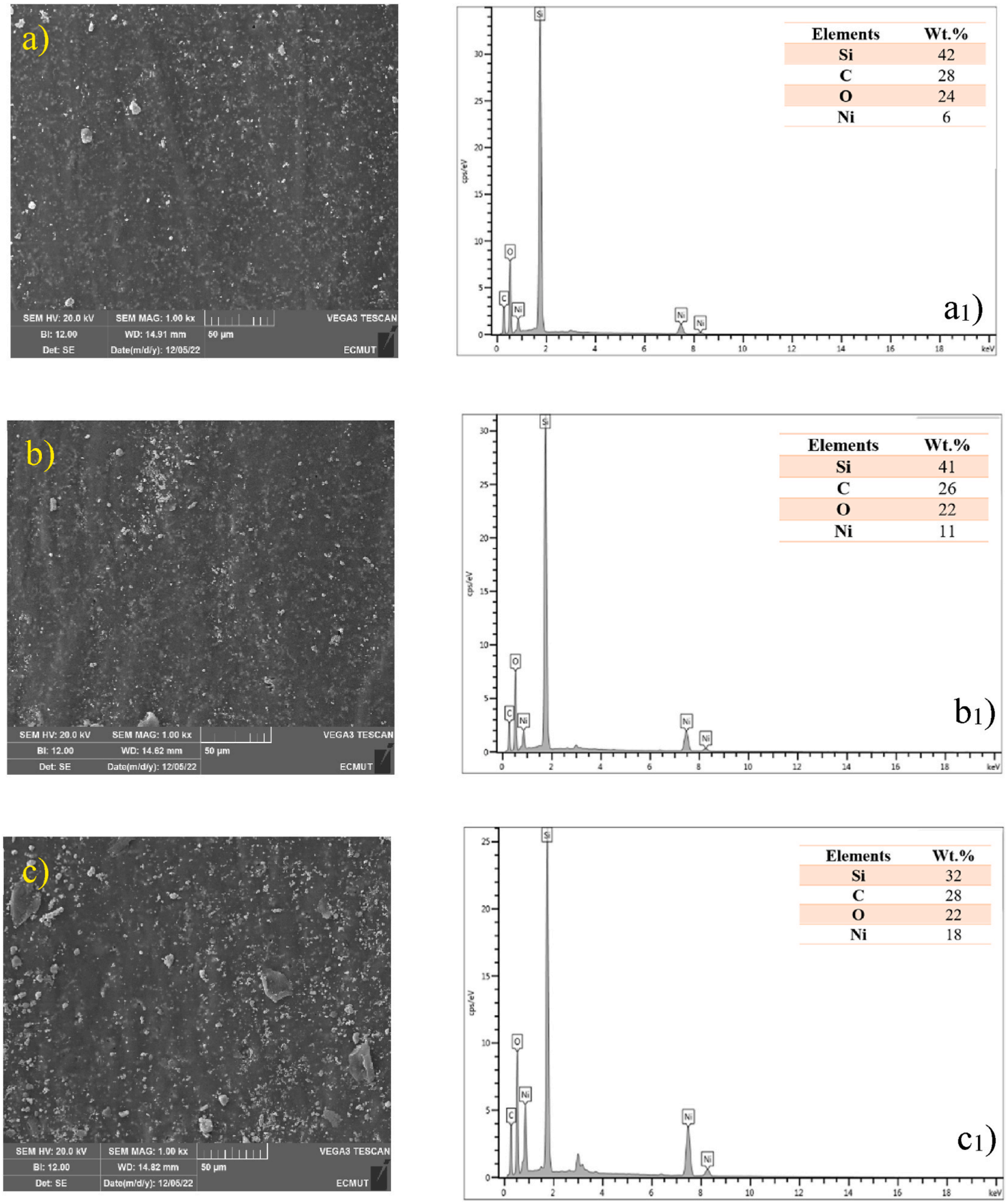

Fig. 4. SEM morphology of conductive gaskets, a) 30 wt% filler, b) 50 wt% filler and c) 70 wt% filler and EDS spectrum of samples a_1) 30 wt% filler, b_1) 50 wt% filler and c_1) 70 wt% filler.

ports. In the notation for S-parameters, the first number in the subscript denotes the responding port, while the second number denotes the incident port. For example, S_{21} refers to the response at port two caused by a signal at port 1.

The quantities SE_T, SE_R, and SE_A are derived from the S-parameters using the following equations:

$$SE_T = -10\log(T) = -10\log|S_{21}|^2 \quad \text{eq.1}$$

$$SE_R = -10\log(1-R) = -10\log\left(1-|S_{11}|^2\right) \quad \text{eq.2}$$

$$SE_A = SE_T - SE_R - SE_M \quad \text{eq.3}$$

The equations presented here involve the transmission coefficient (T) and the reflection coefficient (R). T represents the portion of input power that enters the sample interior, while R represents the portion of input power reflected from the sample surface. It is

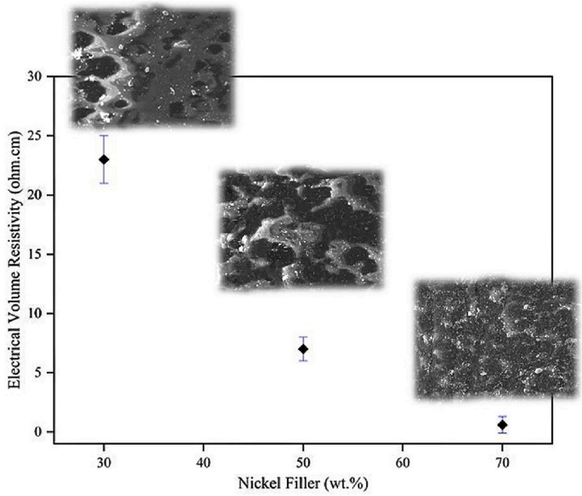

Fig. 5. Variation of volume resistivity of gaskets with the loading of nickel fillers.

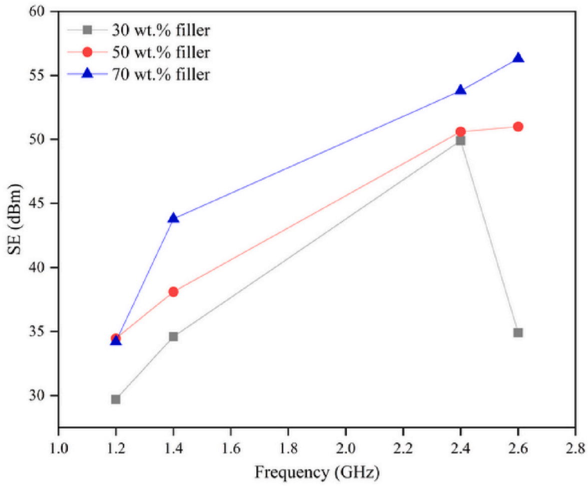

Fig. 6. The shielding effectiveness of gaskets containing different amounts of nickel fillers.

important to report T and R as percents or percentages, and not in dB units. In equation (3), SE_M represents the shielding resulting from multiple reflections within the sample. In practical applications, SE_M is usually negligible when the total shielding (SE_T) is greater than 15 dBm.

The results in Fig. 7(a–c) demonstrate that, regardless of the sample, both SE_T and SE_A increase as the frequency increases. In fact, the highest filler content (70 wt%) leads to SE_T values exceeding 54.64 dB and SE_A values exceeding 40.1 dBm. However, the influence of frequency on both SE_T and SE_A is minimal. Additionally, it is worth noting that SE_A values are significantly higher than SE_R values, indicating that the absorption contribution escalates with frequency [5,8].

4. Conclusion

The present study involves the synthesis of high-quality nickel powder through chemical reduction, which was found to be crystalline and free from impurities, as evidenced by phase analysis. Subsequently, conductive electromagnetic interference (EMI) gaskets were produced by incorporating nickel powders as a filler and peroxide as the crosslinking agent to silicone rubber. Notably, the electrical resistivity of the gaskets was reduced from 23 Ω cm to 0.6 Ω cm as a function of increasing nickel content from 30 to 70 wt percent. Furthermore, the shielding effectiveness of gaskets was found to be significantly enhanced (above 55 dBm) in the frequency range of 1.2–2.6 GHz. These results indicate the potential of the synthesized nickel powder for producing conductive EMI gaskets with improved electrical and electromagnetic shielding properties.

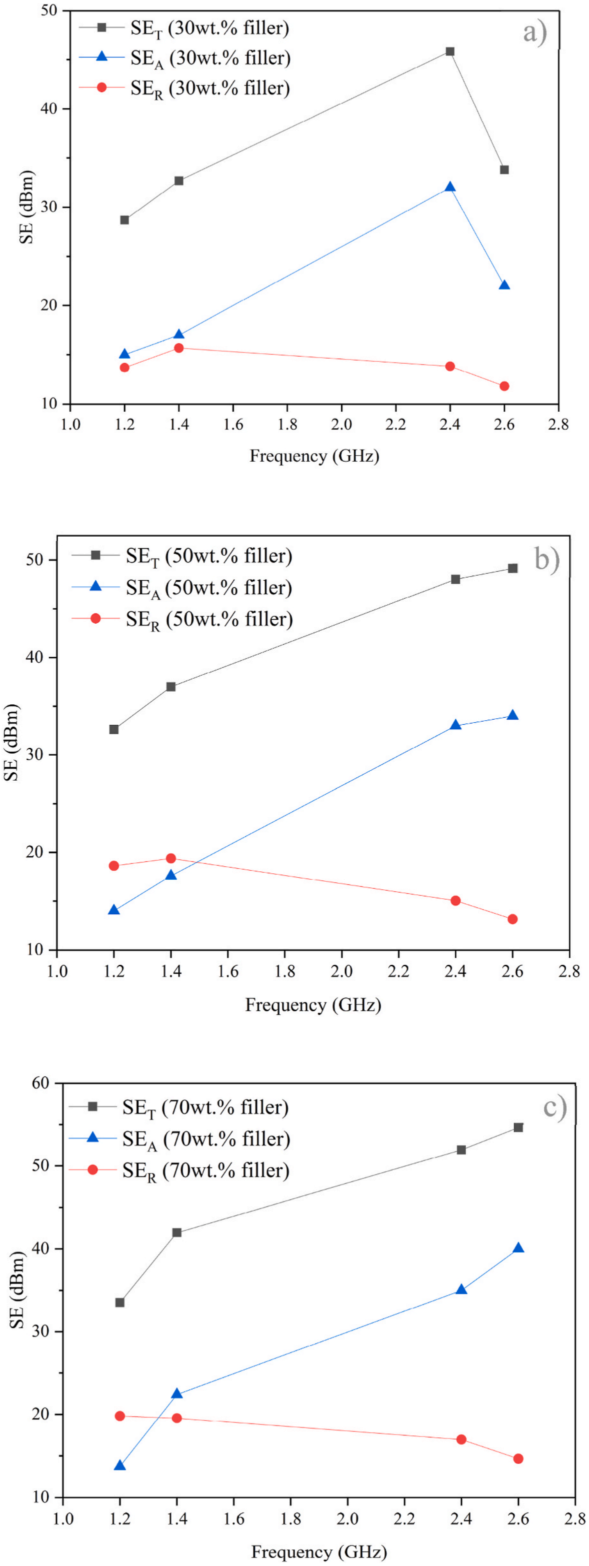

Fig. 7. Shielding results for EMI gaskets (a) SE_T, SE_A and SE_R, each vs. frequency, **a) 30 wt% filler, b) 50 wt% filler and c) 70 wt% filler.**

Additional information

No additional information is available for this paper.

CRediT authorship contribution statement

Atefeh Heidarian: Writing - review & editing, Writing - original draft, Visualization, Validation, Software, Resources, Methodology, Investigation, Funding acquisition, Formal analysis, Data curation, Conceptualization. **Hamed Naderi-Samani:** Writing - review & editing, Writing - original draft, Visualization, Validation, Supervision, Software, Resources, Project administration, Methodology, Investigation, Funding acquisition, Formal analysis, Data curation, Conceptualization. **Reza Shoja Razavi:** Supervision, Investigation, Funding acquisition. **Mahsa Nejad Jabbari:** Visualization, Validation, Supervision, Investigation, Formal analysis, Data curation. **Ehsan Naderi-Samani:** Visualization, Validation, Software, Conceptualization.

Declaration of competing interest

The authors declare that they have no known competing financial interests or personal relationships that could have appeared to influence the work reported in this paper.

References

[1] C. Liu, et al., Lightweight and high-performance electromagnetic radiation shielding composites based on a surface coating of Cu@ Ag nanoflakes on a leather matrix, J. Mater. Chem. C 4 (5) (2016) 914–920.
[2] D. Wanasinghe, F. Aslani, G. Ma, Electromagnetic shielding properties of carbon fiber reinforced cementitious composites, Construct. Build. Mater. 260 (2020) 120439.
[3] A.K. Singh, A. Shishkin, T. Koppel, N. Gupta, A review of porous lightweight composite materials for electromagnetic interference shielding, Compos. Part B Eng. 149 (2018) 188–197.
[4] N. Kozak, et al., Influence of coordination complexes of transition metals on EMI-shielding properties and permeability of polymer blend/carbon nanotube/nickel composites, Compos. Sci. Technol. 200 (2020) 108420.
[5] M. Ozturk, D.D.L. Chung, Enhancing the electromagnetic interference shielding effectiveness of carbon-fiber reinforced cement paste by coating the carbon fiber with nickel, J. Build. Eng. 41 (February) (2021) 102757, https://doi.org/10.1016/j.jobe.2021.102757.
[6] D. Wanasinghe, F. Aslani, A review on recent advancement of electromagnetic interference shielding novel metallic materials and processes, Compos. Part B Eng. 176 (July) (2019) 107207, https://doi.org/10.1016/j.compositesb.2019.107207.
[7] Netic Shielding Effect. Silicone 21 (August) (2011) 93–104.
[8] D.D.L. Chung, Materials for electromagnetic interference shielding, Mater. Chem. Phys. 255 (July) (2020) 123587, https://doi.org/10.1016/j.matchemphys.2020.123587.
[9] O.A. Logutenko, A.I. Titkov, A.M. Vorob'ev, I.K. Shundrina, Y.M. Yukhin, N.Z. Lyakhov, Synthesis of nickel nanoparticles by the reduction of its salts using the modified polyol method in the presence of sodium polyacrylates with various molecular weights, Russ. J. Gen. Chem. 88 (2) (2018) 288–294, https://doi.org/10.1134/S1070363218020160.
[10] R. Eluri, B. Paul, Synthesis of nickel nanoparticles by hydrazine reduction: mechanistic study and continuous flow synthesis, J. Nanoparticle Res. 14 (4) (2012) 1–14, https://doi.org/10.1007/s11051-012-0800-1.
[11] A. Pandey, R. Manivannan, A study on synthesis of nickel nanoparticles using chemical reduction technique, Recent Pat. Nanomed. 5 (1) (2015) 33–37, https://doi.org/10.2174/1877912305666150417232717.
[12] S. Hu, H. Li, X. Chen, C. Zhang, Z. Liu, The electrical conductive effect of nickel-coated graphite/two-component silicone-rubber sealant, J. Wuhan Univ. Technol.-Materials Sci. Ed. 28 (3) (2013) 429–436, https://doi.org/10.1007/s11595-013-0708-3.
[13] G. Cummins, M.P.Y. Desmulliez, Inkjet printing of conductive materials: a review, Circ. World 38 (4) (2012) 193–213, https://doi.org/10.1108/03056121211280413.
[14] H. Guan, D.D.L. Chung, Effect of the planar coil and linear arrangements of continuous carbon fiber tow on the electromagnetic interference shielding effectiveness, with comparison of carbon fibers with and without nickel coating, Carbon N. Y. 152 (2019) 898–908, https://doi.org/10.1016/j.carbon.2019.06.085.